J Sustain Const Mater Technol, Vol. 9, Issue. 1, pp. 11–24, March 2024

Journal of Sustainable Construction Materials and Technologies
Web page info: https://jscmt.yildiz.edu.tr
DOI: 10.47481/jscmt.1406171

JSCMT
Journal of Sustainable Construction Materials and Technologies

Research Article

Research on the long-term strength development of Datça Pozzolan-based geopolymer

Kübra Ekiz BARIŞ*[1], Leyla TANAÇAN[2]

[1]*Department of Architecture and Design, Kocaeli University, İzmit, Türkiye*
[2]*Department of Architecture, İstanbul Technical University, İstanbul, Türkiye*

ARTICLE INFO

Article history
Received: 17 December 2023
Revised: 25 January 2024
Accepted: 02 February 2024

Key words:
Geopolymer, heat curing, long-term curing, natural pozzolan, strength, ultrasound pulse velocity

ABSTRACT

This study examined the influence of long-term curing duration on the properties of geopolymers produced through the geopolymerization reaction between Datça Pozzolan and sodium silicate and potassium hydroxide solutions. The specimens were heat cured at 90 °C, 95±5% RH for 24 h initially and then kept under ambient conditions until the tests were conducted at 7, 90, and 365 days. The results showed that applied initial heat curing was appropriate to achieve high early and long-term strength. Geopolymer mortars with 12.5 M and 2.5 activator ratios had the lowest porosity (20.90%) and the highest ultrasound pulse velocity (UPV) (3.10 km/s), compressive strength (10.57 MPa), and flexural strength (5.20 MPa) after seven days. While the porosity of the identical specimens decreased by up to 15.77%, the UPV, compressive strength and flexural strength increased by 3.37 km/s, 15.32 MPa, and 6.06 MPa, respectively, after 365 days. The physical and mechanical improvement in the first 90 days exceeded 90–365 days. A higher rate of improvement was obtained when the activator ratio was low, i.e., the improvement decreased inversely as the sodium silicate content of the mortar increased. An increasing trend was observed in the plot of compressive strength as a function of UPV, and the slope values presented a strongly related linear function relation.

Cite this article as: Barış, K. E., & Tanaçan, L. (2024). Research on the long-term strength development of Datça Pozzolan-based geopolymer. *J Sustain Const Mater Technol*, 9(1), 11–24.

1. INTRODUCTION

The cement industry is responsible for 5–7% of CO_2 emissions, and the global demand for OPC by 2030 is projected to increase by 216% [1]. In Türkiye, the housing sector consumes 32% of the total energy, and 8.,7% of the total CO_2 emissions originate from cement production [2]. Therefore, the search for low-embodied CO_2 materials is essential for Türkiye. Geopolymers can reduce CO_2 emissions compared with cement production [3]. The geopolymeric reactivity of Datça Pozzolan was investigated in the literature, and the results revealed that it could be used as an aluminosilicate source to produce geopolymer mortars [4]. However, the possibilities of using this material in the building industry should be further investigated toward a carbon-neutral building stock commitment.

The evolution of the geopolymer structure into a semi-crystalline amorphous material and the consequent strength properties of the final product is affected by the curing conditions (curing temperature, duration, humidity), mixture components (precursor and activator type), and mixture design parameters (water/solid ratio, molar ratios of Si/Al, Al/Na, and H_2O/Na_2O). Proper curing conditions prevent high porosity and permeability and, therefore, improve the strength gain of the material. Regardless of the type and dosage of alkali activators, curing below or

***Corresponding author.**
*E-mail address: kubra.ekizbaris@kocaeli.edu.tr

at room temperature (7–20 °C) is not convenient for geopolymers because the beginning of the setting is delayed, and the chemical reaction rate is prolonged [5–9]. Mineral phases in natural pozzolan dissolved in the first three days. The dissolved phases remained 7 and 14 days after the reaction, and the geopolymer matrix continued progressing. At 28 days, the morphology of dense plates, which is related to the polycondensation reaction, produced an interconnected structure, and it was predicted that it would improve over time due to the progress of the geopolymerization reaction [10]. For example, brick powder-based geopolymer cured at 28 and 90 days yielded strengths of 5.3 and 18.7 MPa, respectively [11]. The strength of the red mud and rice husk ash-based geopolymer became almost constant in 35 days (11.7 MPa), and the geopolymer could only gain strength after a certain curing period [12]. Haruna et al. [13] cured high calcium-fly ash-based one-part alkali-activated binders at 25 °C for 365 days. The maximum strength was found after 90 days, and the strength improvement at 180 and 365 days was negligible compared with that at 90 days. The increase in strength beyond 28 days was explained by the formation of fly ash reactions at later ages, which resulted in more calcium alumina silicate hydrate gel production.

Although curing at elevated temperatures is an energy-intensive process, it is particularly crucial in low-calcium aluminosilicate precursors to initiate geopolymerization reactions and enhance the mechanical properties of the final cured products [14]. Elevated temperature curing could overcome the obstacle to further reaction along with improved dissolution of reactive species [5]. An increase in the curing temperature up to 90 °C favors the dissolution of reactive species [15], substantially improves cross-linking in an amorphous structure [14], and increases the compressive strength of the product [6, 16]. According to Naghizadeh et al. [17], the strength development and durability performance of fly ash-based geopolymer concrete (Na_2O/FA>0.09–0.10) cured at 60 °C for 24 h were higher than those of the specimens cured under ambient conditions for 28 days. Another study determined that heat curing at 60 °C for a more extended curing period was beneficial for strength development [18]. According to Bing-hui et al. [19], who investigated the effects of curing temperature (within the range of 20 to 100 °C) on the properties of metakaolin-based geopolymers, elevating the curing temperature increases the activity of hydroxide ions and the dissolution rate of amorphous aluminosilicates; increases polycondensation, polymerization, and reprecipitation processes due to the dehydration of water in the early stage of the geopolymerization reaction; and finally, accelerates the hardening process and improves the physical properties of the geopolymer. However, a curing temperature higher than the appropriate one may negatively affect the properties. For example, Yılmaz et al. [20] determined that curing low-calcium fly ash-based geopolymer mortars above 60 °C for 24, 48, and 72 h decreased the strength of the material. In another study investigated by Yang et al. [21], the mechanical properties of the steel slag-based geopolymer mortar decreased above 60 °C because of the increased shrinkage cracks of the material. Curing temperatures above the optimum one caused rapid setting and restrained the transformation into a compact and tough structure due to the following reactions: The viscosity of the slurry increased rapidly at the initial polycondensation stage. Dissolved ions of aluminate precursors react quickly and increase the setting speed; therefore, the time between the initial and final setting is extremely short. With the rapid coagulation of the slurry, undissolved aluminosilicate particles are covered with this gel, and further dissolution of amorphous phases and solid-state transformation into dense structures is restrained [19]. Zeolite-like crystalline products are formed at higher temperatures (up to 200 °C) [22].

When metakaolin-based geopolymers are cured at temperatures lower than 50 °C, the dissolution and formation of hydroxy species are not complete and insufficient to form the oligomers, leading to lower compressive strength results [23]. However, when pre-cured at 75 °C for three hours, it exhibited improved mechanical properties without diminishing in the long-term curing up to 28 days. However, mixtures of metakaolin and slag cured at the same temperature produced microstructural defects through volume expansion [24]. Aygörmez et al. [25] cured colemanite and metakaolin-based geopolymer mortar at 60 °C for 72 h and allowed it to cure under ambient conditions for 365 days. The strength results were lower at day 365 than at day 14, and it was explained that curing at 60 °C for 72 h positively affected the strength in the early period. However, rapidly developing reaction products adversely affect the material's long-term microstructure and strength properties.

Numerous studies have been conducted on the humidity conditions during the curing of geopolymers. Both natural and artificial-based geopolymers, cured in an oven (RH≤10%) at 70–90 °C, showed visible cracks on the surface of the specimens caused by a substantial loss of moisture and drying shrinkage [10–13, 16, 24–27]. Likewise, the compressive strength of Datça pozzolan-based geopolymer binder was 9.36 MPa after curing at 90 °C under sealed conditions; however, its strength decreased to 5.60 MPa without sealed conditions at the same curing temperature [4]. Therefore, geopolymerization reactions require moisture during the first curing stage to produce a stronger crack-free product [16]. Bondar et al. [28] achieved higher early strength by curing alkali-activated Taftan pozzolan at 60 °C. However, by curing at 40 °C under sealed conditions, higher strength could be obtained in the long term (365 days). In addition, the tests conducted at 28, 90, and 120 days showed a good correlation between ultrasound pulse velocity (UPV) and compressive strength, suggesting that pulse velocity techniques could be successfully used for the estimation of geopolymer strength made with alkali-activated natural pozzolans. Indeed, non-destructive ultrasonic wave technology allows continuous monitoring of a material's reaction process. By the propagation speed of the ultrasound pulse in a material, early-age reaction processes and microstructure development, improvement in rheological properties, setting (due to initial gel formation), hardening and strength development (due to the gradual progression of polymerization/crystallization), and durability properties have been successfully measured [28–32].

Table 1. Chemical analysis of natural Datça Pozzolan

	SiO_2	Al_2O_3	Fe_2O_3	CaO	MgO	P_2O_5	K_2O	Na_2O	TiO_2	MnO_2	Cr_2O_3	NiO
Wt%	75.29	15.99	0.98	1.22	0.62	0.07	3.02	2.21	0.14	0.04	0.005	0.004
	CuO	ZnO	Rb	SrO	Y_2O_3	ZrO_2	Nb_2O_5	BaO	Cl	SO_3	LOI	Total
Wt%	0.002	0.002	0.006	0.015	0.002	0.01	0.001	0.097	0.092	0.1	0.15	100

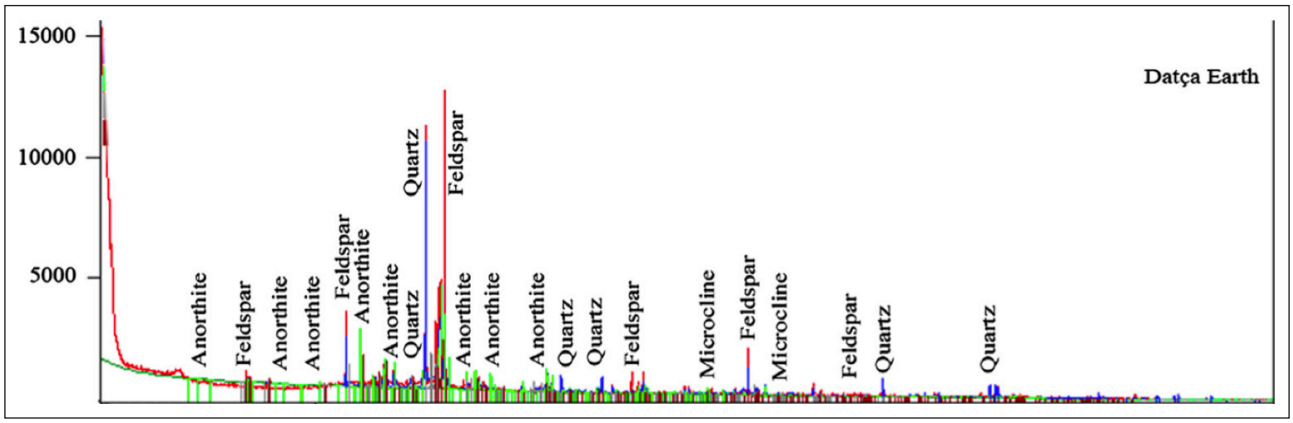

Figure 1. XRD analysis of natural Datça Pozzolan.

If the results are analyzed critically, the strength of the geopolymers cured under ambient conditions continues to increase for up to 90 days. On the other hand, in the geopolymers pre-cured at higher temperatures. However, the early strength increases because of the effect of the temperature. It may decrease in the long term depending on the source precursor. Strength development largely depends on the aluminosilicate precursor and alkali activator type, alkali concentration, activator ratio, curing type, temperature, and curing period. The novelty of this manuscript is that it investigates the development of the properties of natural pozzolan-based geopolymers over the long term by considering the effects of various alkali concentrations and activator ratios. Therefore, the effort to achieve the desired target strength must be determined experimentally for each mixture design. Thus, the objectives of this study are as follows: 1) to investigate the influence of long-term curing on the physical and mechanical properties of heat-cured Datça pozzolan-based geopolymers; 2) to determine the effect of alkali concentration and activator ratio on the long-term microstructural evolution of the geopolymer by evaluating the relationship between UPV and physical and mechanical properties, and 3) to predict the geopolymer strength from UPV.

2. MATERIALS AND METHODS

Natural pozzolan [33], extracted from the Datça Peninsula in Türkiye, was used as an aluminosilicate source to produce geopolymer mortar. It was dried at 55 °C for 24 h and pulverized until a particle size of 95% less than 90 µm was obtained. It has a significantly high specific surface area (5467 cm^2/g) and a specific gravity of 2.52 g/cm^3. The chemical characterization results obtained using an X-ray fluorescence spectrometer (XRF) are presented in Table 1.

As can be seen, the most abundant oxides are pozzolanic oxides (SiO_2 and Al_2O_3), followed by K_2O and Na_2O. It can be accepted as a low-calcium pozzolan (1.22% CaO ≤5%) and classified as a dacitic pozzolan (63–77% SiO_2) because of its 75.2% SiO_2 content [1]. The mineralogical composition (X-ray diffraction, XRD) analysis indicated that the pozzolan consisted mainly of anorthite, quartz, feldspar, microcline, and a compound with an amorphous structure, as shown in Figure 1.

Liquid sodium silicate (Na_2SiO_3) with a 3.24 modulus (SiO_2/Na_2O) and technical-grade potassium hydroxide (KOH) were used for alkaline activation. KOH solutions with 7.5, 10, and 12.5 molarities (M) were prepared by dissolving KOH pellets in distilled water and allowing them to cool before being added to the mixture.

Since this study is based on the previous research of the authors [4], the mixing ratios and initial curing conditions of the first seven days applied in the last study were taken as the basis. The sodium silicate (SS)-to-KOH ratios, termed "activator ratio," were 1.0, 1.5, 2.0, and 2.5. The total alkaline activator-to-binder ratio was kept constant at 0.30 by weight. Standard quartz sand was used with a maximum grain size of 2.0 mm in conformity with TS EN 196-1 [34]. The dry pozzolan/sand ratio was 1/3, and the mortar flow was maintained at 60.

The slurry was cast into prismatic molds with dimensions of 40x40x160 mm. The following curing method was applied: (i) first, curing at 20 °C and 95±5% RH for 24 h, and curing at 90 °C and 95±5% RH for 24 h; (ii) after demolding the specimens, curing at 20 °C and 55±5% RH until testing at 7, 90, and 365 days.

The specimens were coded in [XM-X-X] format: "XM" represents the molarity (M) of KOH, the second group indicates the activator ratio and the third group indicates the curing duration. To ensure reproducibility, three specimens

were prepared for each test; only the compressive strength test was applied to six specimens. The specimens were tested for unit weight (Δ) and specific gravity according to TS EN 1015-10 [35], water absorption under atmospheric pressure (Sa) according to TS EN 13755 [36], dynamic ultrasound velocity (UPV)/Young's modulus of elasticity (MoE) according to TS EN 14579 [37], and flexural (R_f) and compressive (R_c) strengths according to TS EN 196-1 [34].

3. RESULTS AND DISCUSSION

3.1. Effect of Heat Curing on the Properties of Mortars

All test results are given in Table 2, and the physical test results of the specimens cured for seven days are shown in Figure 2.

The porosity (P) and water absorption ratio (S_a) of the material decreased gradually, depending on the increase in the molarities from 7.5, 10 to 12.5 M, as well as the rise in activator ratios varying from 1, 1.5, 2 to 2.5 after seven days of curing. In parallel with these changes, unit weights gradually increased. According to the short error bars, no significant variations were observed in almost all physical properties. In the mortar series of 12.5 M, the water absorption ratio reduced at the fastest rate (0.86 times) on average. The water absorption ratio gives the pore volume ratio of the material to be larger than 0.1 microns that water could penetrate.

On the other hand, open porosity (S_h) is the ratio of open and interconnected pores that water can fill. If (P), (S_a), and (S_h) were analyzed concerning the effect of alkali molarity and activator ratios on pore structure, it could be determined that the micro and gel void ratios (≤0.1 μ) of the (7.5M-1.0–7) and (12.5M-2.5–7) mortars increased from 2% to 20%, respectively, 13 times. An increase in the alkali molarity and alkali activator ratio promoted the formation of a more stable geopolymer gel with lower porosity [38]. However, the pore structure and morphology of the mortars should be further analyzed using mercury intrusion porosimetry (MIP) and scanning electron microscopy equipped with energy-dispersive X-ray spectroscopy (SEM-EDX). The saturation coefficient (SC) denotes the quality of the material in terms of frost resistance and is recommended to be lower than 80% for porous ceramics. All samples produced in this study, even after 365 days, indicated that a frost-resistant material was produced, as shown in Table 2.

The mortars produced in this study were microstructurally monitored using the UPV method. In this method, the ultrasonic pulse is coupled into the material from a transducer and undergoes multiple reflections at the boundaries of the different material phases within the material. A complex system of stress waves is developed that includes both longitudinal and shear waves propagating through the material. The pulse velocity (V) (in km/s or m/s) is given by:

$$V = l / t \quad (1)$$

Where (l) is the path length and (t) is the pulse's time to transverse that length. The pulse velocity (V) of longitudinal stress waves in a material is related to its elastic properties and unit weight according to the following relationship:

$$E_d = 10^5 x V^2 x \Delta / g \quad (2)$$

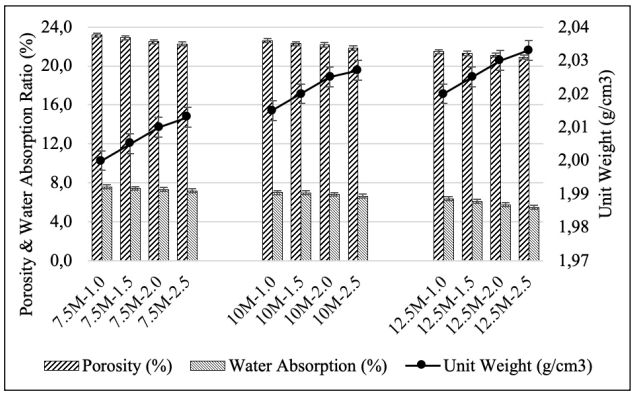

Figure 2. Comparison of the physical properties of mortars with different molarities (7.5, 10, and 12.5) and activator ratios (1, 1.5, 2, and 2.5) after seven days.

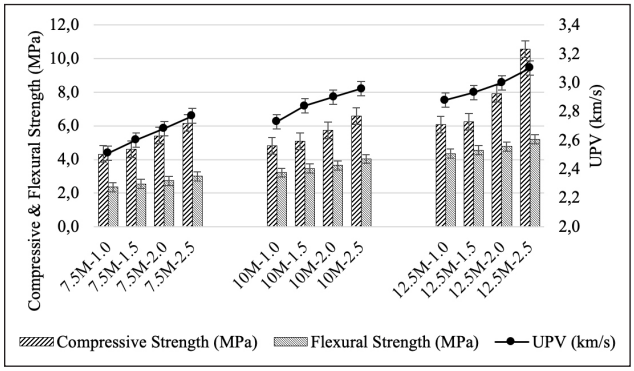

Figure 3. Comparison of the mechanical properties of mortars with different molarities (7.5, 10, and 12.5) and activator ratios (1, 1.5, 2, and 2.5) after seven days.

Where (E_d) is the dynamic modulus of elasticity (MoE), (V) is the pulse velocity, (Δ) is the unit weight of the material, and (g) is the gravitational acceleration (g:9.81m/s).

UPV values were measured on average at 2.64, 2. at 85, and 2.89 km/s, in parallel with the increase in molarity (7.5, 10, and 12.5 M) and activator ratio, UPV increased by 1.1 times on average, respectively. This indicates that the geopolymer evolved toward a more homogeneous structure without cracks or gaps that will reduce the ultrasound velocity by absorption or dispersion. The dynamic modulus of elasticity (MoE) of the material increased in parallel with (UPV) and unit weight (Table 2). MoE values increased by an average of 1.23 times as the molarity of the mortars increased and by an average of 1.20 times as the activator ratio increased.

Moreover, as the molarity concentration increased, the effectiveness of the activator ratio on all properties decreased. The elasticity modulus of cement-lime mortars (binder/sand ratio: 1:3) varies between 40% lime: 23 MPa and 80% lime: 11 MPa, depending on the lime content in the mortar. In this study, very close MoE values between 12.8 and 19.9 MPa were obtained in mortars in 7 days with the effect of heat cure at 90 °C [39]. With the same sand content, the MoE of cement mortars is given as 37.5 MPa. MoE is a measure of the stiffness of a material; in this sense, after seven days, more elastic mortars were produced than cement mortars.

Table 2. Test results of the specimens

Specimen codes of the series	Unit weight (Δ)	Porosity (P) (%)	Open porosity (S_h) (%) (S_a*Δ)	Water absorption (S_a) (%)	Saturation coefficient (SC) (%) (S_h/P)	Ultrasound pulse velocity (UPV) (km/s)	Modulus of elasticity (MoE) (GPa)	Compressive strength (R_c) (MPa)	Flexural strength (R_f) (MPa)
7.5M-1.0-7	2.00	23.18	15.22	7.61	66	2.51	12.84	4.32	2.35
7.5M-1.5-7	2.01	22.90	14.90	7.43	65	2.60	13.81	4.60	2.55
7.5M-2.0-7	2.01	22.50	14.69	7.31	65	2.68	14.71	5.41	2.73
7.5M-2.5-7	2.01	22.25	14.47	7.19	65	2.77	15.74	6.16	3.00
7.5M-1.0-90	2.02	21.40	14.13	7.00	62	2.71	15.12	6.30	3.02
7.5M-1.5-90	2.02	21.12	14.10	6.71	63	2.80	16.18	6.63	3.22
7.5M-2.0-90	2.03	19.91	13.81	6.48	62	2.89	17.30	7.66	3.39
7.5M-2.5-90	2.03	19.36	13.50	6.22	62	3.01	18.82	8.35	3.70
7.5M-1.0-365	2.02	20.90	12.89	6.59	60	2.75	15.78	7.21	3.11
7.5M-1.5-365	2.03	20.14	12.35	6.23	58	2.83	16.82	7.56	3.31
7.5M-2.0-365	2.03	19.27	11.69	6.00	55	2.92	17.95	8.53	3.52
7.5M-2.5-365	2.03	18.67	11.14	5.86	53	3.06	19.81	9.10	3.77
10M-1.0-7	2.02	22.62	14.14	7.01	66	2.73	15.31	4.82	3.21
10M-1.5-7	2,03	22.30	13.59	6.98	64	2.84	16.61	5.10	3.47
10M-2.0-7	2.03	22.17	13.17	6.82	66	2.90	17.36	5.74	3.65
10M-2.5-7	2.04	21.84	12.68	6.66	65	2.96	18.10	6.59	4.03
10M-1.0-90	2.03	20.47	12.24	6.03	60	2.97	18.25	7.03	3.91
10M-1.5-90	2.04	20.08	11.99	5.89	60	3.05	19.30	7.41	4.07
10M-2.0-90	2.04	19.23	11.67	5.71	61	3.10	20.01	8.02	4.32
10M-2.5-90	2.05	18.91	11,39	5.56	60	3.20	21.38	8.76	4.60
10M-1.0-365	2.04	19.82	11.02	5.75	57	3.00	18.85	7.90	3.97
10M-1.5-365	2.04	19.01	10.77	5.63	58	3.09	20.07	8.25	4.15
10M-2.0-365	2.05	18.28	9.92	5.49	56	3.15	20.96	8.78	4.44
10M-2.5-365	2.06	17.31	9.31	5.34	56	3.28	22.83	9.50	4.79
12.5M-1.0-7	2.05	21.47	13.49	6.38	65	2.88	17.08	6.07	4.35
12.5M-1.5-7	2.06	21.29	12.83	6.10	64	2.93	17.72	6.25	4.56
12.5M-2.0-7	2.07	21.10	12.39	5.76	64	3.00	18.62	7.90	4.77
12.5M-2.5-7	2.08	20.90	12.16	5.48	65	3.10	19.92	10.57	5.20
12.5M-1.0-90	2.06	19.50	11.82	5.41	60	3.12	20.21	9.25	5.20
12.5M-1.5-90	2.06	18.47	11.61	5.28	61	3.16	20.77	9.71	5.38
12.5M-2.0-90	2.07	17.62	11.38	4.84	62	3.25	22.07	11.35	5.57
12.5M-2.5-90	2.08	16.50	11.12	4.53	64	3.31	22.95	14.57	5.88
12.5M-1.0-365	2.06	18.90	10.40	5.05	55	3.21	21.64	10.13	5.38
12.5M-1.5-365	2.07	18.02	9.52	4.61	53	3.25	22.23	10.55	5.56
12.5M-2.0-365	2.08	16.93	9.17	4.42	54	3.32	23.31	12.00	5.75
12.5M-2.5-365	2.09	15.77	8.53	4.09	54	3.37	24.13	15.32	6.06

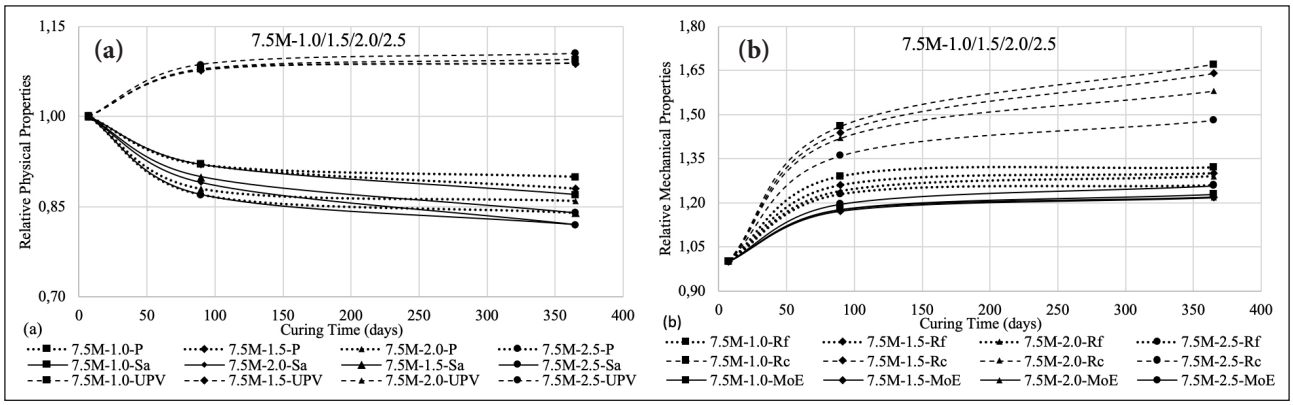

Figure 4. Graph of relative properties as a function of curing duration: **(a)** physical properties (P, S_a, Δ) at 7.5 M; **(b)** mechanical properties (R_c, R_f, UPV) at 7.5 M.

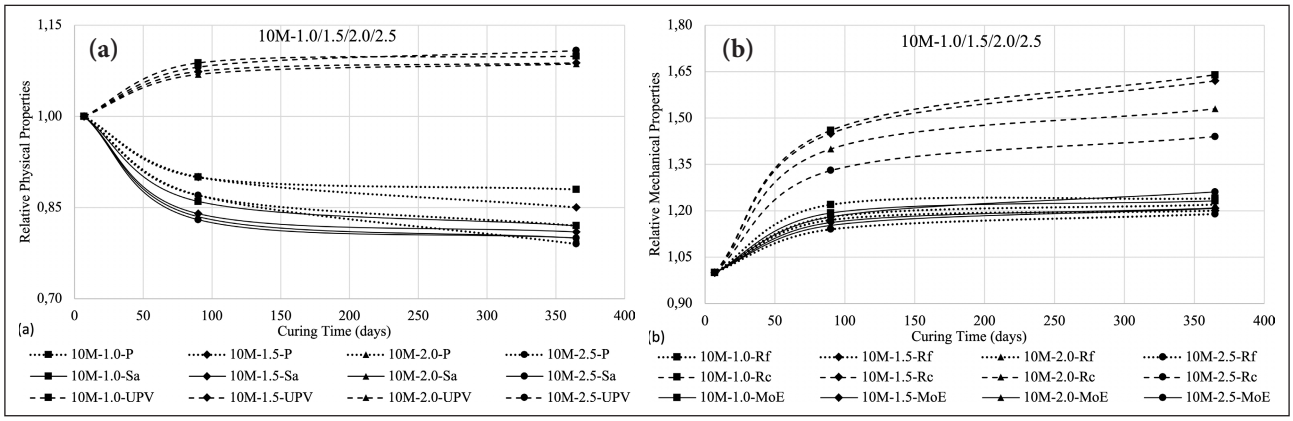

Figure 5. Graph of relative properties as a function of curing duration: **(a)** physical properties (P, S_a, Δ) at 10 M; **(b)** mechanical properties (R_c, R_f, UPV) at 10 M.

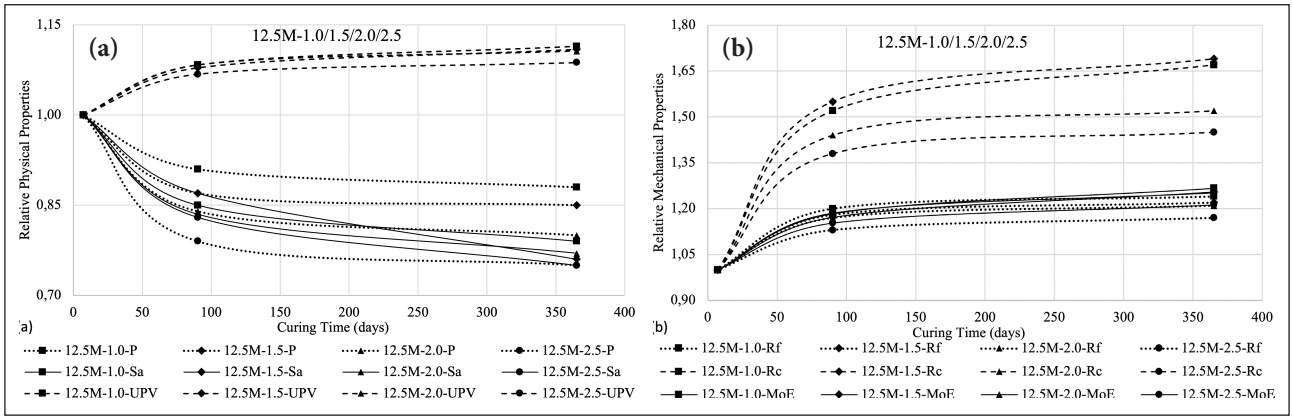

Figure 6. Graph of relative properties as a function of curing duration: **(a)** physical properties (P, S_a, Δ) at 12.5 M; **(b)** mechanical properties (R_c, R_f, UPV) at 12.5 M.

The rising trend observed in the material's mechanical strength after seven days of curing was parallel to its physical properties (Fig. 3). The shorter error bars in Figure 3 indicate less uncertainty in the test results. According to the 7-day compressive strength (R_c) results, an increase in (R_c) was determined depending on the rise in both molarities (7.5, 10, 12.5) and activator ratio (1.0, 1.5, 2.0, 2.5). On the 7-day, the (R_c) of 12.5 M was 1.50 and 1.38 times higher than R_c) values of 7.5 and 10 M, respectively. Therefore, the 12.5 M concentration resulted in mechanical properties at seven days. This improvement, which was detected by increasing the molarity of the activator, may be explained by the fact that higher concentrations of alkali hydroxides enhance the dissolution of Datça pozzolan as an aluminosilicate source. The higher amount of dissolved Si and Al in the reaction zone favors the development of a continuous polycondensation reaction [40] with a three-dimensional structure (NASH gel).

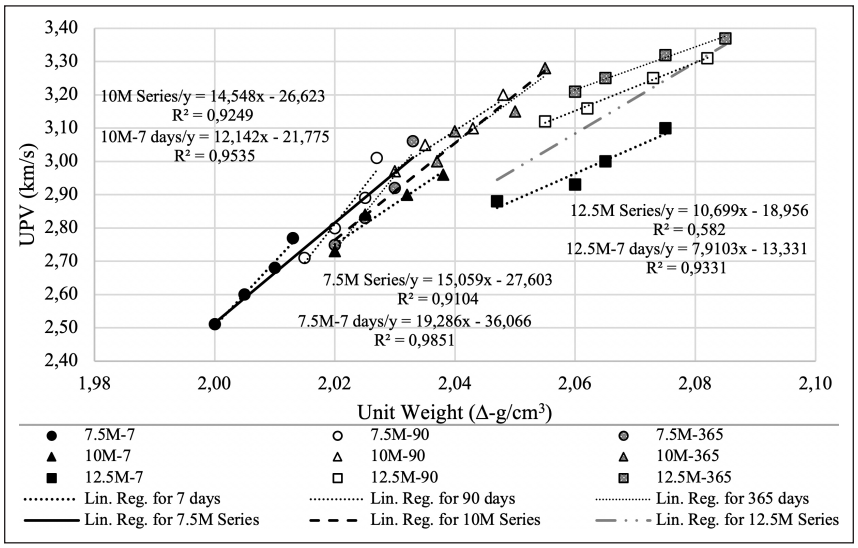

Figure 7. Ultrasound pulse velocities (UPV) of the mortar series (7.5, 10, and 12.5 M) as functions of unit weight (Δ).

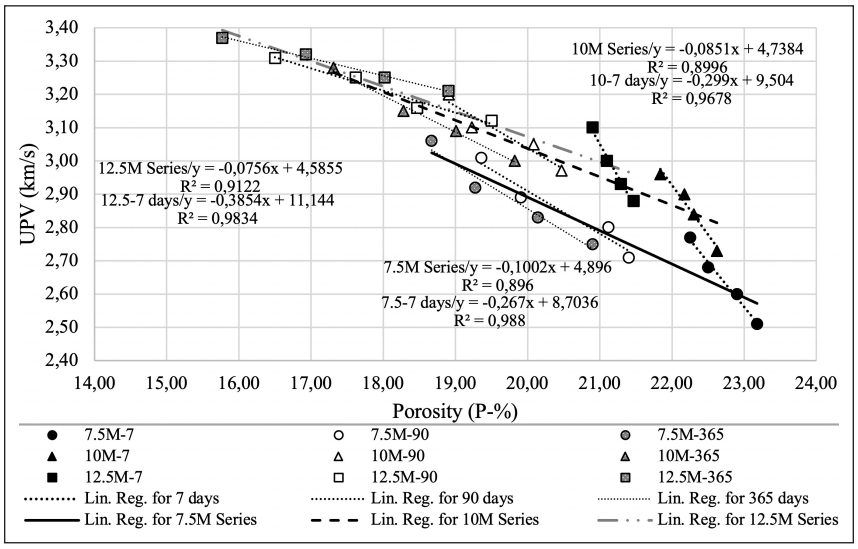

Figure 8. Ultrasound pulse velocities (UPV) of the mortar series (7.5, 10, and 12.5 M) as functions of porosity (P).

The increase in compressive strength (R_c) due to the higher activator ratio (SS/K), mainly when the activator ratio is 2 and 2.5, indicates a higher sodium silicate (SS) content in the mixture and can be explained as follows: (i) SS enhances the dissolution rate of Si and Al in the aluminosilicate source; (ii) Al ions dissolve quickly in the alkali medium because the Al–O bonds of the aluminosilicate source are weaker than the Si–O bonds. As a result, more Si ions in the reaction medium may increase the degree of geopolymerization [41]. In addition, more SS in the mixture also leads to stronger ion-pair formation, which leads to more long-chain silicate oligomers. The longer-chain silicate oligomers mean the NASH gel is more easily formed [42]. Furthermore, a geopolymer binder with a more homogeneous structure with high silica availability was obtained in the early stages [38]. Thus, a higher activator ratio of the geopolymer mixture is important to support the development of geopolymerization reactions on day 7. As a result, heat curing at 90 °C benefited the strength development by improving the physical properties of the mortars after seven days.

3.2. Effect of Curing Duration on the Properties of Mortars

The geopolymer mortars' relative physical and mechanical properties with 7.5, 10, and 12.5 molarities and activator ratios of 1, 1.5, 2, and 2.5 as functions of curing duration are shown in Figures 4–6.

Effect of Curing Duration on the Activator Ratio: As the curing time progressed, the improvement in the physical and mechanical properties of the mortars with lower activator ratios was greater in all mortars with 7.5, 10, and 12.5 M concentrations. Because the properties of the mortar with a high activator ratio already reached their highest value at the end of the 7-day cure, the increase in the long term slowed down. That is, the densification and continuous formation of the geopolymer matrix increased as the activator ratio decreased. While this improvement was more effective in the first 90 days, it lost its efficiency between 90 and 365 days. Despite the relatively low rate of improvement in the physical properties at all activator

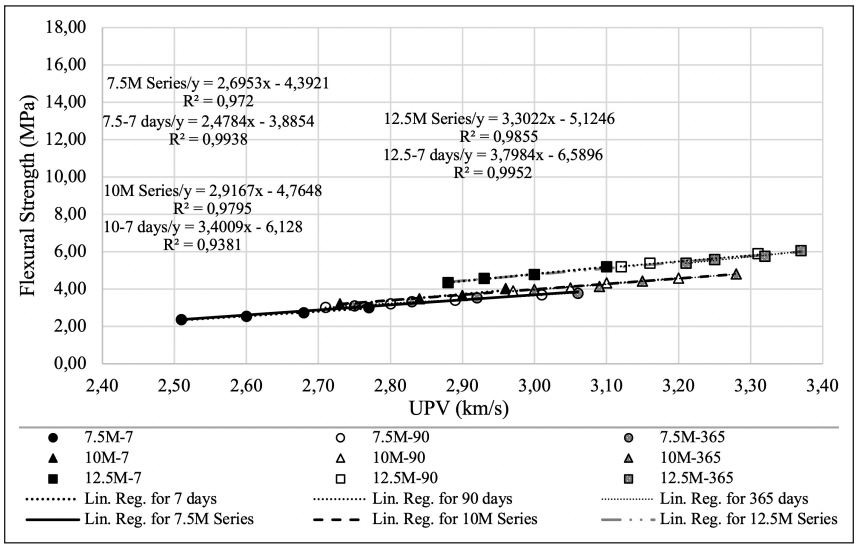

Figure 9. Flexural strengths (R_f) of the mortar series (7.5, 10, and 12.5 M) as functions of (UPV).

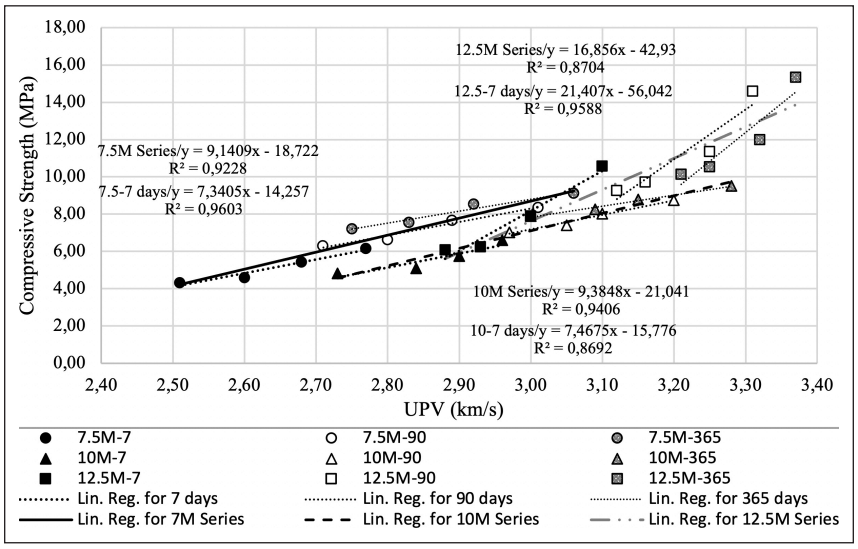

Figure 10. Compressive strengths (R_c) of the mortar series (7.5, 10, and 12.5 M) functions of (UPV).

ratios, a significant increase in the compressive strengths was observed. This increased rate, again, which was higher at lower activator ratios, took lower values in parallel with the increase in activator ratios. The strength of a material is closely related to its fine-grained microstructure and low porosity. The inverse relationship between the porosity, UPV, water absorption, and the strengths of all mortars was obtained accordingly.

Although the time-dependent increase rate in the 12.5 M and 2.5 activator ratio specimen, which gave the highest mechanical properties in 7-day curing, was at the lowest level, its mechanical properties at 90 and 365 days were still the highest. In other words, the increased efficiency in the first seven days in the development of geopolymerization reactions also positively reflected the results obtained in the later period.

Effect of Curing Duration on Alkali Concentration: The changes detected in the properties of the geopolymer mortars revealed that the material transformed into a more compact microstructure and improved structurally over time. However, the improvement rate in mortar properties was negligible between 90 and 365 days, compared with 7 to 90 days. These findings are incompatible with the research results of colemanite and metakaolin-based geopolymer mortar, which claim that rapidly developing reaction products by pre-curing at 60 °C for 72 h have a negative influence on the long-term microstructure and strength properties of the material [25]. This emphasizes that the aluminosilicate source, alkaline reactants, and their ratios play a role in developing the internal structure of geopolymers and the curing effect.

As expected from the decrease in porosity, the UPV values of 7.5, 10, and 12.5 M geopolymer mortars on the 365 days increased by an average of 1.09, 1.10, and 1.10 times compared with those obtained on day 7. While the average UPV values obtained in 7 days were 2.64, 2.86, and 2.98 km/s, respectively, these values increased to an average of 2.89, 3.13, and 3.29 km/s in 365 days. UPV values of less than three km/s indicate that the strength is very low due to excess voids [43]. UPV values within the scope of this

Table 3. Comparison of calculated and experimental results of compressive strengths (R_c)

Specimen code	R_c calc. (MPa)	R_c exp. (MPa)	Diff. (%)	Specimen code	R_c calc. (MPa)	R_c exp. (MPa)	Diff. (%)	Specimen code	R_c calc. (MPa)	R_c exp. (MPa)	Diff. (%)
7.5M-1.0-7	4.22	4.32	2.34	10M-1.0-7	4.57	4.82	5.55	12.5M-1.0-7	5.63	6.07	7.88
7.5M-1.5-7	5.04	4.60	8.80	10M-1.5-7	5.60	5.10	8.90	12.5M-1.5-7	6.47	6.25	3.40
7.5M-2.0-7	5.78	5.41	6.32	10M-2.0-7	6.16	5.74	6.83	12.5M-2.0-7	7.65	7.90	3.27
7.5M-2.5-7	6.60	6.16	6.64	10M-2.5-7	6.72	6.59	1.99	12.5M-2.5-7	9.34	10.57	13.22
7.5M-1.0-90	6.05	6.30	4.14	10M-1.0-90	6.82	7.03	3.12	12.5M-1.0-90	9.67	9.25	4.37
7.5M-1.5-90	6.87	6.63	3.52	10M-1.5-90	7.57	7.41	2.09	12.5M-1.5-90	10.35	9.71	6.16
7.5M-2.0-90	7.69	7.66	0.45	10M-2.0-90	8.04	8.02	0.21	12.5M-2.0-90	11.87	11.35	4.34
7.5M-2.5-90	8.79	8.35	5.02	10M-2.5-90	8.98	8.76	2.40	12.5M-2.5-90	12.88	14.57	13.15
7.5M-1.0-365	6.42	7.21	12.3	10M-1.0-365	7.10	7.90	11.2	12.5M-1.0-365	11.19	10.13	9.48
7.5M-1.5-365	7.15	7.56	5.79	10M-1.5-365	7.94	8.25	3.86	12.5M-1.5-365	11.87	10.55	11.08
7.5M-2.0-365	7.97	8.53	7.04	10M-2.0-365	8.51	8.78	3.22	12.5M-2.0-365	13.05	12.00	8.01
7.5M-2.5-365	9.25	9.10	1.60	10M-2.5-365	9.73	9.50	2.32	12.5M-2.5-365	13.89	15.32	10.31
Mean	6.82	6.82		Mean	7.31	7.33		Mean	10.32	10.31	
Standard deviation (s)	1.47	1.53		Standard deviation (s)	1.45	1.50		Standard deviation (s)	2.66	2.84	
Coefficient of variation (CV)	21.55	22.43		Coefficient of variation (CV)	19.83	20.46		Coefficient of variation (CV)	25.77	27.54	

study were determined to be in the range of 2.85–3.21 km/s even after 90 days of curing. The increase in UPV, MoE, and strength of the samples depending on the curing time may indicate the formation of a three-dimensional amorphous aluminosilicate structure (NASH gel) that fills the voids and bridges the unreacted pozzolan particles [13]. However, different morphologies were also detected, where a clear distinction was observed between the gel and unreacted particles, unlike the spherical shape of fly ash, which might cause the structure to become denser or more porous [9].

90% of the compressive strength could be obtained in one day in low-calcium FA-based geopolymers cured at 80–90 °C; however, when the same samples were cured under ambient conditions for a long time, the strength increased, similar to that of OPC cement. Therefore, long-term strength could be achieved under all curing conditions, and increasing the curing temperature only accelerates the change over time [44]. However, in our study, the compressive strength obtained in 365 days increased 1.56 times on average for all mortar series of 7.5, 10, and 12.5 M compared with the compressive strength obtained in the first seven days. Therefore, in the same mortars, with the triggering effect of curing at 90 °C (RH: 95%) for 24 h, the strengths obtained in the first seven days constituted only 64% on average of the strengths in 365 days. With the effect of the elapsed curing time, the highest strength development was obtained at the highest molar concentration ratio.

It is indicated for brittle materials that the flexural strength is often approximately 0.10 of the compressive strength [45]. The R_f/R_c ratios of 7.5, 10, and 12.5 M mortars were 0.51, 0.66, and 0.64 on average in 7 days, respectively, and decreased to an average of 0.42, 0.51, and 0.48 in 365 days, respectively. Over time, this decrease in the ratio indicates that the curing duration has a greater effect on the compressive strength and that the geopolymer has evolved into a more fragile structure. However, mortars still exhibit elastic behavior.

3.3. Effects of Alkali Concentration and Activator Ratio on the Long-Term Microstructural Evolution of Geopolymers

The non-destructive and continuous character of the investigations with ultrasound pulse velocity (UPV) makes it possible to take continuous measurements of the hydration kinetics, to indicate variations in the mix composition due to the mix formulation, and to assess the strength development of materials [46]. On the other hand, the compressive strength of a material is the most essential mechanical property and notably influences other properties, including density, porosity, flexural strength, and modulus of elasticity. However, the UPV technique cannot determine the strength of cementitious systems made of different materials consisting of various ingredients and proportions [47]. Therefore, to estimate the strengths of geopolymers from ultrasound velocity, the effects of alkali concentrations and activator ratios on long-term microstructural evolution were interpreted by correlating UPV with other macro properties such as porosity, unit weight, compressive strength, and flexural strength. The analysis was performed based on 7 and 365 days, as seven days represent the effect of heat curing on the geopolymerization of the mortar series, while 365 days represent the effect of the entire curing time.

Effect of Unit Weight and Porosity on the UPV: Ultrasound pulse velocities (UPV) of all mortar series, based on their different molarities (7.5, 10, and 12.5 M) as functions of unit weight (Δ) after 7, 90, and 365 days of curing, are depicted in Figure 7.

According to the (UPV) development observed after seven days of curing, as the molarities and activator ratios of the mortar series of 7.5, 10, and 12.5 M increased, (UPV) s increased as functions of unit weight (Δ). The slopes of the regression lines of each mortar series show how the changes influence the (UPV)s of the series in their (Δ)s. Accordingly, the mortar series of 7.5 M was the most affected, followed by the 10 and 12.5 M mortar series. The slopes of the regression lines reduced slowly toward higher molarities on the order of 7.5 M (m_7:19), 10 M (m_7:12), and 12.5 M (m_7:8).

Parallel to the increase in the activator ratio from 1 to 2.5, all properties, including (UPV) gradually improved. Initial heat curing accelerates hydroxide ions' activity and the amorphous aluminosilicates' dissolution rate. However, the initial release of Al is faster than that of Si, and the dissolved ions of aluminate precursors react with any silicate initially provided by the activating solution, leading to the formation of aluminosilicate gel phases. Therefore, sodium silicate solutions as activators have better mechanical properties than alkali hydroxide alone. However, as the molar concentrations gradually increased toward 10 and 12.5 M, the efficiency of the SS may decrease progressively. At low molar concentrations, the quantity of the alkali solution is the lowest, and the Si ions provided by SS become more efficient in the mixture. This might be why a higher rate of improvement was obtained in the long term when the activator ratio was low; that is, the improvement decreased inversely as the sodium silicate content of the mortar increased.

The same trend was also detected in the long-term curing results. The slopes of the mortar series of 7.5 and 10 M were almost the same (m_{365}:15), indicating similar (UPV) development as functions of (Δ) in time. On the other hand, the mortar series of 12.5 M had the lowest slope (12.5M m_{365}) in 365 days, indicating that their (UPV)s were least influenced by (Δ)s over time. Increasing the activator ratio from 1 to 2.5 increased the UPV at all molarities, but the most significant increase was in the 7.5 M series, which was 1.22-fold. Towards 10 and 12.5 M, the improvement rate decreased by 1.20 and 1.17 times, respectively. However, the unit weight increase at each molarity was only 1.02 times.

The rate of improvement in the (UPV)s of the mortar series of 7.5 M became 0.79 times slower at the longer curing duration of 365 days than that of the values obtained at seven days (m_7:19>m_{365}:15). On the other hand, both slopes of the mortar series of 10 M and 12.5 M increased 1.20 (m_7:12<m_{365}:14.5) and 1.35 times (m_7:7.9<m_{365}:10.6) respectively. Hence, in the long term, better structural improvements were detected for the mortar series of 10 and 12.5 M than in seven days. However, the (Δ) improvement was only in the 2.02–2.09 g range/cm^3, which can be considered negligible.

Although the regression lines of the mortar series of 7.5 and 10 M had strong correlation coefficients (R^2>0.90) between (UPV)s and (Δ)s at both 7 and 365 days, the mortar series of 12.5 M only had a strong correlation (R^2:0.93) at seven days; at later days of curing duration, the correlation coefficient between these properties dropped by 0.62 times (R^2:0.58) in 365 days. This significant decrease in the correlation coefficient may be because the 7-day UPV values of the 12.5 M series remain much lower than the 90 and 365-day values. For example, at the same unit weight value (2.06 g/cm^3), UPV values were obtained as 2.93 km/s in 7 days, 3.16 km/s in 90 days, and 3.21 km/h in 365 days. In other words, while the 90-day increase rate was 1.08 times the 7-day value, the increase rate between 90 and 365 days was lower, 1.01 times. Figure 8 shows the (UPV) values of all mortar series based on their different molarities (7.5, 10, and 12.5 M) as functions of porosity (P) after 7, 90, and 365 days.

There is an inverse relationship between these two properties, as expected. As the (P)s of the mortar series increased, the (UPV) values decreased in the descending order of 12.5, 10, and 7.5 M. The increment of activator ratios from 1 to 2.5 also positively influenced the reduction of P values. Again, in the 7.5 M mortars, the rate rose in porosity, and the rate rose in UPV was the highest. After seven days of curing, even the negative slopes of the regression lines for each mortar series were almost the same (m_7:-0.3) and strongly correlated with an average of R^2=0.97. The same inverse trend was observed for long-term curing. The slopes of all mortar series were almost the same (m_{365}:-0.08), indicating similar (UPV) development as functions of (P) over time. The regression lines of each molarity also define the existence of a strong correlation ($7.5M_{365}$ and $10M_{365}$: R^2=0.89 and 12.5 M_{365}: R^2=0.91) between the two properties.

The negative slopes of the regression lines of the (UPV) s of all mortar series as functions of (P) at seven days dropped by 0.27 times (m_7:-0.3> m_{365}:-0.08) on average in the long-term curing of 365 days. Although the decrease in the porosity of the mortars changed the UPV to a lower level, mortars continued to develop their geopolymerization at a slower rate. Densification of solid phases increased the ultrasound pulse velocity of the material; however, since the reaction rate declined gradually, the UPV increased at a slower rate in the long term.

Effect of UPV on the Mechanical Properties: The flexural strengths (R_f) of all mortar series, based on their different molarities (7.5, 10, and 12.5 M) as functions of (UPV) after 7, 90, and 365 days of curing, are depicted in Figure 9.

As the molarities and activator ratios of the mortar series increased, (R_f) increased as a function of (UPV). The slopes of the regression lines of all mortar series were almost identical and in strong correlation (7.5 M: m_7:2.4, R^2=0.99; 10 M: m_7:3.4, R^2=0.93; 12.5 M m_7:3.7, R^2=0.99) after seven days. The same trend was also detected in long-term curing. The slopes of the regression lines obtained for the 7.5 M (m_{365}:2.7), 10 M (m_{365}:2.9), and 12.5 M (m_{365}:3.3) mortar series were also close to each other with a strong correlation after 365 days (7.5M: R^2: 0.97, 10M: R^2: 0.98 and 12.5M: R^2: 0.99).

Compared with the change in UPV, the increase in flexural strength (R_f) at a lower rate than the compressive strength (R_c) may indicate that the material has turned into a more brittle structure.

The compressive strengths (R_c) of all mortar series (7.5, 10, and 12.5 M) as functions of (UPV) after 7, 90, and 365 days of curing are depicted in Figure 10. The compressive strength is a good indicator of the degree of geopolymerization.

According to the (R_c) development after seven days, as the molarities and activator ratios of the mortars increased, (R_c)s increased as functions of (UPV) for each of the mortar series of 7.5, 10, and 12.5 M. The slopes of the regression lines for the mortar series of 7.5 M and 10 M were almost identical (7.5M and 10M: m_7:7.4) but lower than the slope of the mortar series of 12.5 M (12.5M: m_7:21.4); the higher slope indicates a higher rate of initial strength development as a function of UPV. The same trend was observed in the long term. The slopes of the regression lines of the mortar series of 7.5 M and 10 M were compatible (7.5 M and 10 M: m_{365}: 9), indicating the existence of a similar solid-state development in (R_c). In addition, the magnitude of the correlation coefficients was relatively high (7.5 M36: R^2: 0.92 and 10 M_{365}: R^2: 0.94).

On the other hand, the mortar series of 12.5 M had the highest slope and the lowest (correlation coefficient 12.5 M: m_{365}: 16.8, R^2: 0.87) in the long term. The reason for this decrease was the sudden increase in the compressive strength of the sample coded (12.5 M-2.5) in 90 and 365 days. However, despite this decrease, it is still 0.87, and the relationship between the two variables is generally considered strong when the "R^2" value is larger than 0.7.

At the same speed as ultrasound, the 7.5 M series with the lowest molar concentration is higher than 10 M. At the end of the 365 days, the compressive strengths of 7.5 M and 10 M become almost equal, while 7.5 M remains more porous. In geopolymers, higher strength can be achieved with a more porous structure. Similarly, a study comparing natural pozzolan-based geopolymer and OPC concrete observed that the UPV values of both materials increased as the curing time increased. Still, the UPV of geopolymer mortars remained lower at the same or higher compressive strengths than concrete [28]. On the other hand, the 12.5 M series maintains its already high compressive strength and relatively tight pore structure in 365 days.

At 365 days, the correlation coefficients between UPV and other properties decreased slightly, except for the slight increase observed for the UPV-R_c and UPV-R_f relationship of the 10 M series. This may imply that the geopolymerization of the mortars occurred very quickly because of the curing effect at 90 °C, and a sufficiently dense structure was formed after seven days. The fact that this process took place in a closed environment and the subsequent curing at ambient temperature for a relatively short period may have improved the correlation between the mortar properties. The last stage of the reaction process, solid-state transformation, involves the continual arrangement of the gel toward three-dimensional geopolymer networks and requires long-term termination. It might have been affected by slight ambient humidity and temperature changes, causing the relationship between properties to change relatively.

The regression lines of the mortar series at 7.5 M (m_7: 7.3 and m_{365}: 9.1) and 10 M (m_7: 7.4 and m_{365}: 9.3) have almost the same slopes at both curing times. The slope of the regression line of 12.5 M drops by 0.79 times at their 365-day curing time (m_7: 21.4 and m_{365}: 16.8). This indicates the occurrence of a lower rate of geopolymerization reaction at curing times longer than seven days for the 12.5 M mortars. It may be concluded from the similar trends of the regression lines at both curing durations (at seven 365 days-day) of each mortar series of 7.5, 10, and 12.5 M that there is a mechanical and physical improvement with time. This may show that the material's compressive strength (R_c) could be estimated through its (UPV) for the mortars under consideration in this study.

When all mortar types at 365 days are considered, the linear correlation between compressive strength (R_c) and (UPV) (R_c= f(v)) can be expressed by the following equation:

$$R_c = a \times V + b \quad (3)$$

"a" gives the slope (m) of the regression lines, which change to 9.14 (for 7.5 M), 9.38 (for 10 M), and 16.86 (for 12.5). "b" is 18.7, 21.04, and 42.93 for 7.5, 10, and 12.5 M mortars, respectively, as expressed by the following formulas:

$$7.5M/R_c = 9.14 \times V - 18.72 \quad (4)$$

$$10M/R_c = 9.38 \times V - 21.04 \quad (5)$$

$$12.5M/R_c = 16.86 \times V - 42.93 \quad (6)$$

There is an inverse V (UPV) - porosity (P) relationship with a high level of correlation in all mortar series (m_{365}:-0.08, R^2=0.90); hence, not only the mechanical properties but also the pore structures improve.

By considering Equations 4, 5, and 6 given above as representative of the compressive strength (R_c)–(V) relationship of the mortar series of 7.5, 10, and 12.5 molarities, the experimental values of V (UPV) of all the specimens, as shown in Table 2, were used to estimate the compressive strength. The estimated strength values were compared with the measured experimental values (Table 3). The standard deviation (s) and coefficient of variation (CV) values for 7.5, 10, and 12.5 M series were found to be (1.47–21.55), (1.45–19.83), and (2.66–25.77) respectively. (CV) of the 10 M, which is 19.83%, indicates that the "fitting" is most satisfactory. According to the compressive strength (R_c) values calculated for each mortar type, there is an approximately two-fold increment in 365 days compared to 7 days: 7.5M=2.19, 10M=2.13, and 12.5M=2.46.

Suppose the (UPV) of 3 km/s, accepted as the quality limit in concrete, is also taken as a limit value for the geopolymer mortars produced in this study. The geopolymer mortars with different molarities and activator ratios can be selected based on their expected performance. Accordingly, the range of physical and mechanical properties above three km/s (UPV) may be given as follows:

- Unit weight (Δ) ranges from 2.03–2.09 g/cm^3
- Porosity (P) varies between 15.77 and 21.10% (9.01–25.84% for geopolymers)
- Open porosity (S_h) varies between 8.53 and 13.50%
- Water absorption (S_a) varies between 4.09 and 6.22% (8–18% for bricks)
- The saturation coefficient (SC) varies between 53 and 62% (<80%)
- Ultrasound pulse velocity (UPV) varies between 3.00 and 3.37 km/s
- The modulus of elasticity (MoE) varies between 18.1 and 24.13 GPa (11–23 GPa for cement-lime mortars (1:3)
- Compressive strength (R_c) varies between 7.41 and 15.32 MPa (≥10 MPa for hydraulic cement)
- Flexural strength (R_f) varies between 3.70 and 6.06 MPa (1.5–3.5 MPa for concrete) [48].

Geopolymer concrete has a high environmental impact on categories other than global warming due to the heavy effect of the production of sodium silicate solution [49]. Hence, selecting mortar types with lower molarities and activator ratios produced within the scope of the study that fulfill the required performance is possible because of the positive effect of curing duration on the properties of geopolymer mortars proven in this study.

4. CONCLUSION

In line with the results obtained throughout the study, the following remarks can be made:

- The Earth of Datça, as a natural pozzolan precursor, has promising characteristics for use as a geopolymer mortar and should be encouraged for practical use as a green building material.
- The initial heat curing regime (24 h at 90 °C) is appropriate for the natural pozzolan-based geopolymer considered in this study because it facilitates the early-age reaction process without restricting the transformation to a compact microstructure in the long term. Moreover, it provides some advantages for practical purposes, such as shortening of demoulding time and early development of strength.
- The initial heat-curing regime had a positive effect on strength development in the early period as well as in the long term. The microstructure and strength properties of the geopolymer continued to progress for up to 365 days. There was an almost twofold improvement after 365 days. The improvement rate between 90 and 365 days was negligible compared with the 7–90 days.
- The rate of increase in the physical and mechanical properties was higher when the activator ratio was low (1.0 and 1.5). In other words, the rate of improvement in the properties decreased inversely with increasing sodium silicate content of the mortar.
- Geopolymer mortars with 12.5 M and 2.5 activator ratios had the highest mechanical properties after 7 and 365 days. However, because of the heavy environmental impact of sodium silicate solution production, selecting geopolymer mortars with lower molarities and activator ratios became possible when considering the positive influence of curing duration on the microstructure of the geopolymers, as proven in this research.
- An increasing trend was observed in the plot of compressive strengths as functions of UPV parallel with the increase in the alkali content of the geopolymer, and the slope values presented a strongly related linear function relation. Finally, the outcomes of this study provide a possible method to assess the strength of natural pozzolan-based geopolymers from ultrasound pulse velocity measurements.
- In this study, the variations in the solid-state transformation of the mortars were monitored by ultrasound and evaluated along with the physical and mechanical properties. However, further research is recommended using advanced measurement techniques to examine mortars' morphology and microstructure development.

ACKNOWLEDGEMENTS

The authors gratefully acknowledge the assistance of İbrahim Öztürk from the Building Materials Laboratory, ITU, Faculty of Architecture.

ETHICS

There are no ethical issues with the publication of this manuscript.

DATA AVAILABILITY STATEMENT

The authors confirm that the data that supports the findings of this study are available within the article. Raw data that support the finding of this study are available from the corresponding author, upon reasonable request.

CONFLICT OF INTEREST

The authors declare that they have no conflict of interest.

FINANCIAL DISCLOSURE

The authors declared that this study has received no financial support.

USE OF AI FOR WRITING ASSISTANCE

Not declared.

PEER-REVIEW

Externally peer-reviewed.

REFERENCES

[1] Robayo-Salazar, R. A., & de Gutiérrez, R. M. (2018). Natural volcanic pozzolans as an available raw material for alkali-activated materials in the foreseeable future: A review. *Constr Build Mater, 189*, 109–118. [CrossRef]

[2] Tanaçan, L., Kaya, K., & Yıldırım, E. (2022). Sustainable building material and technology [Sürdürülebilir yapı malzemesi ve teknoloji]. *İTÜ Vakıf Derg, 90*, 14–23.

[3] Singh, N. B., & Middendorf, B. (2020). Geopolymers as an alternative to portland cement: An overview. *Constr Build Mater, 237*, 117455. [CrossRef]

[4] Barış, K. E., & Tanaçan, L. (2021). Improving the geopolymeric reactivity of Earth of Datça as a natural pozzolan in developing green binder. *J Build Eng, 41*, 102760. [CrossRef]

[5] Jiang, D., Shi, C., & Zhang, Z. (2022). Recent progress in understanding the setting and hardening of alkali-activated slag (AAS) materials. *Cem Concr Comp, 134*, 104795. [CrossRef]

[6] Wang, K., Shah, S. P., & Mishulovich, A. (2004). Effects of curing temperature and NaOH addition on hydration and strength development of clinker-free CKD-fly ash binders. *Cem Concr Res, 34*(2), 299–309. [CrossRef]

[7] Nath, P., & Sarker, P. K. (2015). Use of OPC to improve the setting and early strength properties of low calcium fly ash geopolymer concrete cured at room temperature. *Cem Concr Comp, 55*, 205–214. [CrossRef]

[8] Hardjito, D., Wallah, S. E., Sumajouw, D. M. J., & Rangan, B. V. (2004). On the development of fly ash-based geopolymer concrete. *ACI Mater J, 101*, 467–472. [CrossRef]

[9] Djobo, J. N. Y., Elimbi, A., Tchakouté, H. K., & Kumar, S. (2016). Volcanic ash-based geopolymer cements/concretes: The current state of the art and perspectives. *Environ Sci Pollut Res, 24*, 4433–4446. [CrossRef]

[10] González-García, D. M., Téllez-Jurado, L., Jiménez-Álvarez, F. J., Zarazua-Villalobos, L., & Balmori-Ramírez, H. (2022). Evolution of a natural pozzolan-based geopolymer alkalized in the presence of sodium or potassium silicate/hydroxide solution. *Constr Build Mater, 321*, 126305. [CrossRef]

[11] Tuyan, M., Andiç-Çakir, O., & Ramyar, K. (2018). Effect of alkali activator concentration and curing condition on strength and microstructure of waste clay brick powder-based geopolymer. *Compos Part B Eng, 135*, 242–252. [CrossRef]

[12] He, J., Jie, Y., Zhang, J., Yu, Y., & Zhang, G. (2013). Synthesis and characterization of red mud and rice husk ash-based geopolymer composites. *Cem Concr Comp, 37*, 108–118. [CrossRef]

[13] Haruna, S., Mohammed, B. S., Wahab, M., Kankia, M. U., Amran, M., & Gora, A. M. (2021). Long-term strength development of fly ash-based one-part alkali-activated binders. *Materials, 14*(15), 4160. [CrossRef]

[14] Athira, V. S., Bahurudeen, A., Saljas, M., & Jayachandran, K. (2021). Influence of different curing methods on mechanical and durability properties of alkali activated binders. *Constr Build Mater, 299*, 123963. [CrossRef]

[15] Heah, C. Y., Kamarudin, H., Mustafa Al Bakri, A. M., Binhussain, M., Luqman, M., Khairul Nizar, I., Ruzaidi, C. M., & Liew, Y. M. (2011). Effect of curing profile on kaolin-based geopolymers. *Phys Procedia, 22*, 305–311. [CrossRef]

[16] Chindaprasirt, P., Chareerat, T., & Sirivivatnanon, V. (2007). Workability and strength of coarse high calcium fly ash geopolymer. *Cem Concr Comp, 29*(3), 224–229. [CrossRef]

[17] Naghizadeh, A., Ekolu, S. O., Tchadjie, L. N., & Solomon, F. (2023). Long-term strength development and durability index quality of ambient-cured fly ash geopolymer concretes. *Constr Build Mater, 374*, 130899. [CrossRef]

[18] Raut, A. N., Murmu, A. L., & Alomayri, T. (2023). Physico-mechanical and thermal behavior of prolong heat cured geopolymer blocks. *Constr Build Mater, 370*, 130309. [CrossRef]

[19] Bing-hui, M., Zhu, H., Xue-min, C., Yan, H., & Si-yu, G. (2014). Effect of curing temperature on geopolymerization of metakaolin-based geopolymers. *Appl Clay Sci, 99*, 144–148. [CrossRef]

[20] Yılmaz, A., Degirmenci, F. N., & Aygörmez, Y. (2023). Effect of initial curing conditions on the durability performance of low-calcium fly ash-based geopolymer mortars. *Boletín de la Soc Española de Cerámica y Vidrio, 2023*, 398. [CrossRef]

[21] Yang, X., Wu, S., Xu, S., Chen, B., Chen, D., Wang, F., Jiang, J., Fan, L., & Tu, L. (2024). Effects of GBFS content and curing methods on the working performance and microstructure of ternary geopolymers based on high-content steel slag. *Constr Build Mater, 410*, 134128. [CrossRef]

[22] Ferone, C., Colangelo, F., Cioffi, R., Montagnaro, F., & Santoro, L. (2011). Mechanical performances of weathered coal fly ash based geopolymer bricks. *Procedia Eng, 21*, 745–752. [CrossRef]

[23] Muñiz-Villarreal, M. S., Manzano-Ramírez, A., Sampieri-Bulbarela, S., Ramón Gasca-Tirado, J., Reyes-Araiza, J. L., Rubio-Ávalos, J. C., Pérez-Bueno, J. J., Apatiga, L. M., Zaldivar-Cadena, A., & Amigó-Borrás, V. (2011). The effect of temperature on the geopolymerization process of a metakaolin-based geopolymer. *Mater Lett, 65*(6), 995–998. [CrossRef]

[24] Kim, H., & Kim, Y. (2013). Relationship between compressive strength of geo-polymers and pre-curing conditions. *Appl Microscopy, 43*(4), 155–163. [CrossRef]

[25] Aygörmez, Y., Canpolat, O., & Al-Mashhadani, M. M. (2020). A survey on one year strength performance of reinforced geopolymer composites. *Constr Build Mater, 264*, 120267. [CrossRef]

[26] Zuhua, Z., Xiao, Y., Huajun, Z., & Yue, C. (2009). Role of water in the synthesis of calcined kaolin-based geopolymer. *Appl Clay Sci, 43*(2), 218–223. [CrossRef]

[27] Perera, D. S., Uchida, O., Vance, E. R., & Finnie, K. S. (2006). Influence of curing schedule on the integrity of geopolymers. *J Mater Sci, 42*, 3099–3106. [CrossRef]

[28] Bondar, D., Lynsdale, C. J., Milestone, N. B., Hassani, N., & Ramezanianpour, A. A. (2011). Engineering properties of alkali-activated natural pozzolan concrete. *ACI Mater J, 108*(1), 1–9. [CrossRef]

[29] Dai, X., Ren, Q., Aydin, S., Yardimci, M. Y., & De Schutter, G. (2023). Accelerating the reaction process of sodium carbonate-activated slag mixtures with the incorporation of a small addition of sodium hydroxide/sodium silicate. *Cem Concr Comp, 141*, 105118. [CrossRef]

[30] Chen, W., Li, Y., Shen, P., & Shui, Z. (2013). Microstructural development of hydrating portland cement paste at early ages investigated with non-destructive methods and numerical simulation. *J Nondestruct Eval, 32*, 228–237. [CrossRef]

[31] Azarsa, P., & Gupta, R. (2017). Electrical resistivity of concrete for durability evaluation: A review. *Adv Mater Sci Eng*, 8453095, 1–30. [CrossRef]

[32] Dai, X., Aydin, S., Yardimci, M. Y., Lesage, K., & De Schutter, G. (2022). Early age reaction, rheological properties and pore solution chemistry of NaOH-activated slag mixtures. *Cem Concr Comp, 133*, 104715. [CrossRef]

[33] Barış, K. E., & Tanaçan, L. (2017). Earth of Datça: Development of pozzolanic activity with steam curing. *Constr Build Mater, 139*, 212–220. [CrossRef]

[34] TS EN 196-1. (2009). Standard Specification for Methods of Testing Cement – Part 1: Determination of Strength. Ankara, TC: Turkish Standard Institution.

[35] TS EN 1015-10. (2001). Standard Specification for Methods of Test for Mortar for Masonry – Part 10: Determination of Dry Bulk Density of Hardened Mortar. Ankara, TC: Turkish Standard Institution.

[36] TS EN 13755. (2014). Standard Specification for Natural Stone Test Methods – Determination of Water Absorption at Atmospheric Pressure. Ankara, TC: Turkish Standard Institution.

[37] TS EN 14579. (2015). Standard Specification for Natural Stone Test Methods – Determination of Sound Speed Propagation. Ankara, TC: Turkish Standard Institution.

[38] Tchadjie, L. N., & Ekolu, S. O. (2017). Enhancing the reactivity of aluminosilicate materials toward geopolymer synthesis. *J Mater Sci, 53*, 4709–4733. [CrossRef]

[39] Kubica, J., & Gasiorowski, S. A. (2010). Mortar selection in design practice - description of the problems, solutions and requirements. *Archit Civ Eng Environ, 3*, 53–61.

[40] Panagiotopoulou, C. H., Kontori, E., Perraki, T. H., & Kakali, G. (2006). Dissolution of aluminosilicate minerals and by-products in alkaline media. *J Mater Sci, 42*, 2967–2973. [CrossRef]

[41] Nadoushan, M. J., & Ramezanianpour, A. A. (2016). The effect of type and concentration of activators on flowability and compressive strength of natural pozzolan and slag-based geopolymers. *Constr Build Mater, 111*, 337–347. [CrossRef]

[42] Xu, H., & Van Deventer, J. S. J. (2000). The geopolymerisation of alumino-silicate minerals. *Int J Miner Process, 59*(3), 247–266. [CrossRef]

[43] Postacıoğlu, B. (1986). Beton - Bağlayıcı Maddeler - Agregalar-2. Cilt. Istanbul, TC: Teknik Kitaplar Yayınevi.

[44] Farooq, F., Jin, X., Javed, M. F., Akbar, A., Shah, M. I., Aslam, F., & Alyousef, R. (2021). Geopolymer concrete as sustainable material: A state of the art review. *Constr Build Mater, 306*, 124762. [CrossRef]

[45] Carter, G. W., Cannor, A. M., & Mansell, D. S. (1982). Properties of bricks incorporating underground rice husks. *Build Environ, 17*(4), 284–291. [CrossRef]

[46] Tanaçan, L., Kurugöl, S., & Ersoy, H. Y. (2009). Investigation of ultrasonic pulse velocity-strength relationship of lime-pozzolan mortars. Fourth International ECOMATERIALS Symposium, Bayamo, Cuba.

[47] Demirboğa, R., Türkmen, I., & Karakoç, M. B. (2004). Relationship between ultrasonic velocity and compressive strength for high-volume mineral-admixtured concrete. *Cem Concr Res, 34*(12), 2329–2336. [CrossRef]

[48] Akman, S. (1990). Yapı Malzemeleri, 2nd ed. İstanbul, TC: ITÜ Matbaası.

[49] Habert, G., d'Espinose de Lacaillerie, J. B., & Roussel, N. (2011). An environmental evaluation of geopolymer based concrete production: Reviewing current research trends. *J Clean Prod, 19*(11), 1229–1238. [CrossRef]